

An Interactive Shader for Natural Diffraction Gratings

Bachelorarbeit

der Philosophisch-naturwissenschaftlichen Fakultät
der Universität Bern

vorgelegt von

Michael Single

2014

Leiter der Arbeit:
Prof. Dr. Matthias Zwicker
Institut für Informatik und angewandte Mathematik

Abstract

In nature color production is the result of physical interaction of light with a surface's nanostructure. In his pioneering work, Stam developed limited reflection models based on wave optics, capturing the effect of diffraction on very regular surface structures. We propose an adaption of his BRDF model such that it can handle complex natural gratings. On top of this, we describe a technique for interactively rendering diffraction effects, as a result of physical interaction of light with biological nanostructures such as snake skins. As input data, our method uses discrete height fields of natural gratings acquired by using atomic force microscopy (AFM). Based on Taylor Series approximation we leverages precomputation to achieve interactive rendering performance (about 5-15 fps). We demonstrate results of our approach using surface nanostructures of different snake species applied on a measured snake geometry. Lastly, we evaluate the quality of our method by a comparison of the maxima for peak viewing angles using the data produced by our method against the maxima resulting by the grating equation.

Contents

1	Implementation	1
1.1	Precomputations in Matlab	2
1.2	Java Renderer	6
1.3	GLSL Diffraction Shader	7
1.3.1	Vertex Shader	7
1.3.2	Fragment Shader	11
1.4	Technical Details	16
1.4.1	Texture Lookup	16
1.4.2	Texture Blending	18
1.4.3	Color Transformation	18
1.5	Discussion	19
1.5.1	Comparison: per Fragment-vs. per Vertex-Shading	19
1.5.2	Optimization of Fragment Shading: NMM Approach	19
1.5.3	The PQ Shading Approach	20
2	Results	23
2.1	BRDF maps	23
2.2	Snake surface geometries	32
	List of Tables	38
	List of Figures	38
	List of Algorithms	39
	Bibliography	40

Chapter 1

Evaluation and data acquisition

1.1 Data Acquisition

Our goal is to perform physically accurate simulations of diffraction effects on natural gratings. As for every simulation, its outcome highly depends on the provided input data we also require measurements¹ of real natural gratings. For that purpose, samples of skins of *Xenopeltis* and *Elaphe* snake species were fixed on a glass plate and then, by using an Atomic Force Microscope (AFM), their surface topography was measured and stored as grayscale images, indicating the depth. In general, an ADM is a microscope that uses a tiny probe mounted on a cantilever to scan the surface of an object. The probe is extremely close to the surface, but does not touch it. As the probe traverses the surface, attractive and repulsive forces arising between it and the atoms on the surface induce forces on the probe that bend the cantilever. The amount of bending is measured and recorded, providing a map of the atoms on the surface. Atomic force microscopes are a very high-resolution type of scanning probe microscopy, with demonstrated resolution on the order of fractions of a nanometer, more than 1000 times better than the optical diffraction limit.

1.2 Diffraction Gratings

In order to evaluate the quality of our simulations, it is important to understand what a diffraction grating actually is. An idealised diffraction grating like in figure ?? is made of a large number of parallel, evenly spaced slits in an opaque medium. In general, if the spacing between slits is wider than the wavelength of the incoming light, then the better we can observe how the light is diffracted on the grating. Simply speaking, each slit in the grating acts as a point light source from which light spreads and propagates in all directions. According to Huygen's Principle the outgoing light may have a different outgoing angle as it had initially. Figure ?? illustrates this behaviour for a monochromatic light source passing through a grating and shows that the outgoing angle will be different from the incident angle. Hence, the diffracted light is composed of the sum of interfering wave components emanating from each slit in the grating.

¹All measured data has been provided by the Laboratory of Artificial and Natural Evolution at Geneva - Website: www.lanevol.org

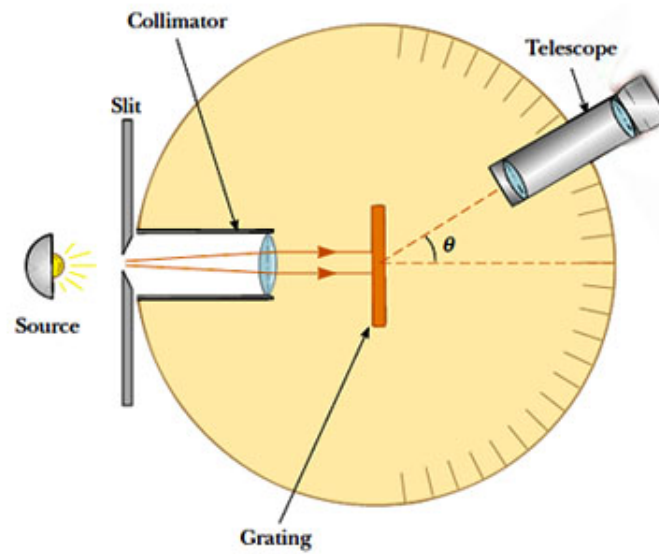


Figure 1.1: Spectrometer: When a beam of monochromatic light passes through a grating placed in a spectrometer, images of the sources can be seen through the telescope at different angles.

Suppose that a monochromatic light source is directed at the grating, parallel to its axis as shown in figure ???. Let the distance between successive slits be equal the value d .

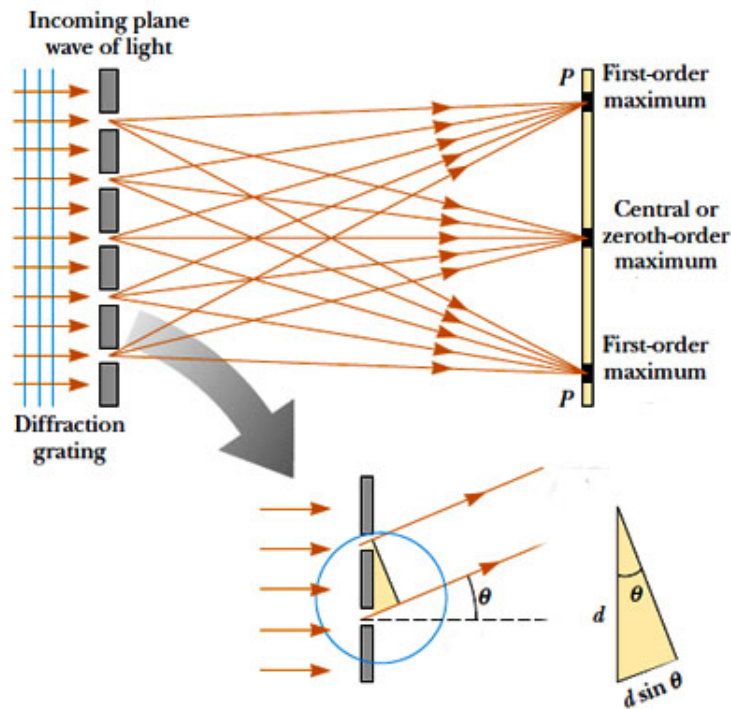


Figure 1.2: Light directed to parallel to grating:

The observable diffraction pattern is the result of interference effects among outgoing wavelets according to Huygen's Principle. The path difference between waves from any two adjacent slits can be derived by drawing a perpendicular line between the parallel waves. Applying some trigonometry, this path difference is $d \sin(\theta)$. If the path difference equals one wavelength or a multiple of the wave's wavelength, the emerging, reflected waves from all slits will be in phase and a bright line will be observed at that point. Therefore, the condition for maxima in the interference pattern at the angle θ is:

$$d \sin(\theta) = m\lambda \quad (1.1)$$

where $m \in \mathbb{N}_0$ is the order of diffraction. Because d is very small for a diffraction grating, a beam of monochromatic light passing through a diffraction grating is split into very narrow bright fringes at large angles θ .

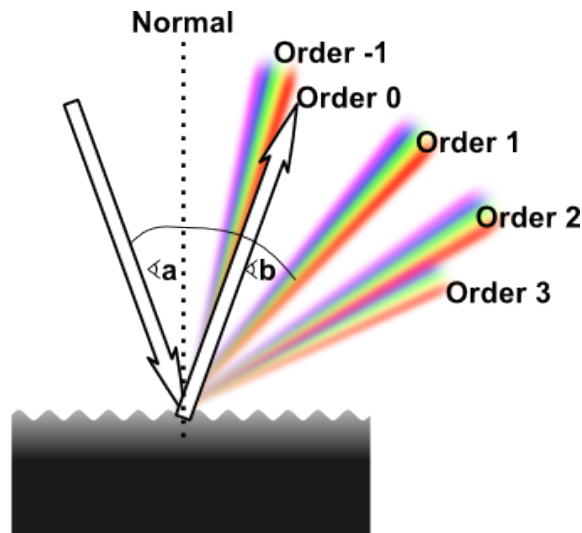


Figure 1.3: Different Orders of diffraction

When a narrow beam of white light is directed at a diffraction grating along its axis, instead of a monochromatic bright fringe, a set of colored spectra are observed on both sides of the central white band as shown in figure ??.

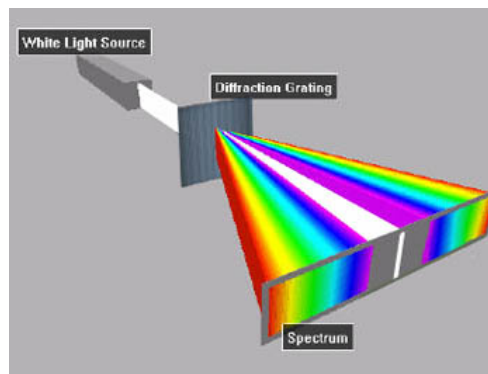


Figure 1.4: White Light beam causes coloured diffraction spectra

Since the angle θ increases with wavelength λ , red light, which has the longest wavelength, is diffracted through the largest angle. Similarly violet light has the shortest wavelength and is therefore diffracted the least. This relationship between angle and wavelength is illustrated in figure ??. Thus, white light is split into its component colors from violet to red light. The spectrum is repeated in the different orders of diffraction, emphasizing certain colors differently, depending on their order of diffraction like shown in figure ??. Note that only the zero order spectrum is pure white. Figure ?? shows the relative intensity resulting when a beam of light hits a diffraction grating for different number of periods. From the graph we recognise that the more slits a grating has, the sharper more slopes the function of intensity gets. This is similar like saying that, the more periods a grating has, the sharper the diffracted color spectrum gets like shown in figure ??.

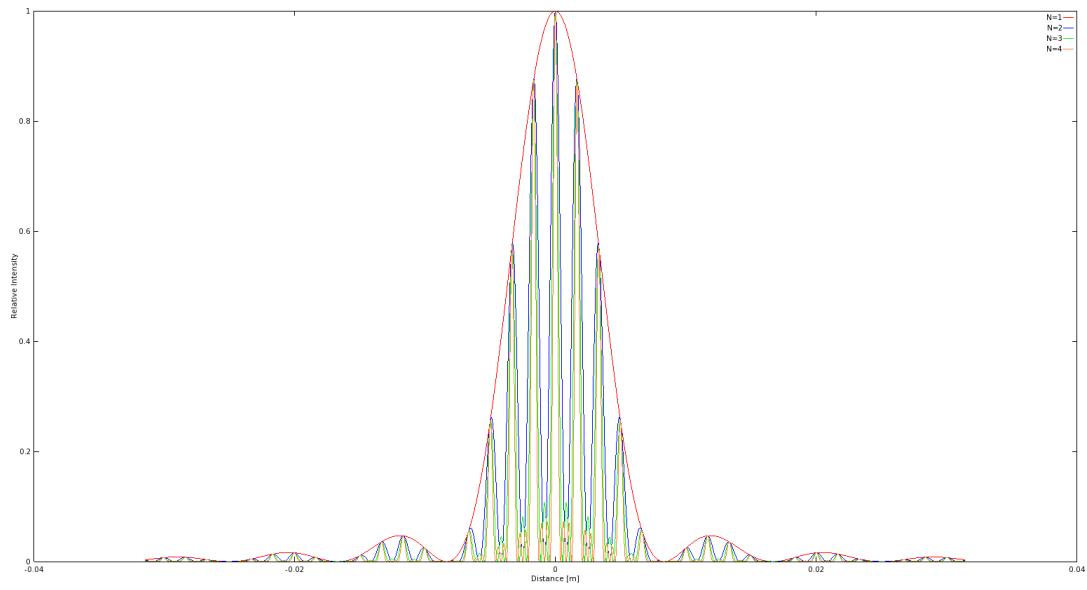
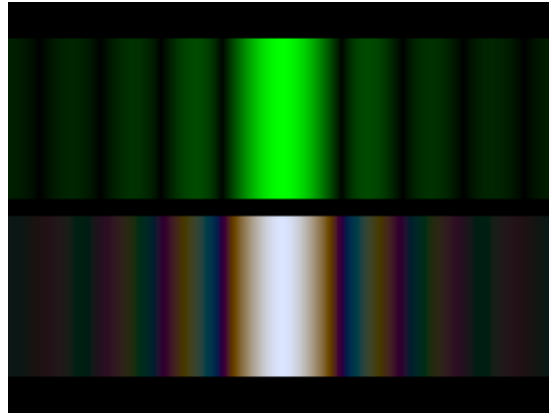
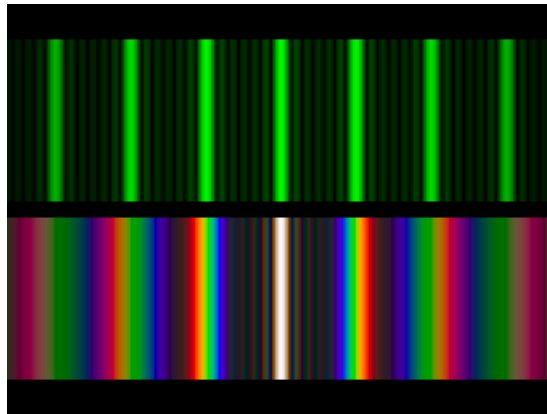


Figure 1.5: Relative intensities of a diffracted beam of light at wavelength $\lambda = 500nm$ on a grating for different number of periods N width slit width of 30 microns and slit separation of 0.15 mm each. The viewer is 0.5m apart from the grating.



(a) one slit



(b) seven slits

Figure 1.6: Difference of diffraction pattern between a monochromatic (top) and a white (bottom) light spectra for different number of slits.

1.3 Evaluation

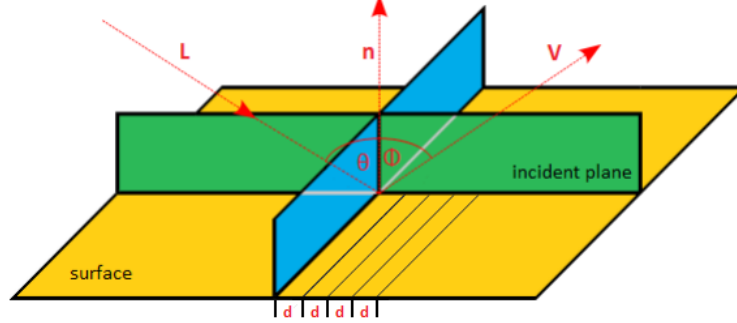


Figure 1.7: Experimental setup for evaluation: A light beam with direction L hits the surface, representing a grating pattern with periodicity d , at the incident plane relative to the surface normal n at angle θ and emerges at angle ϕ with direction V .

The physical reliability of our BRDF models has been verified by applying those on various patches which are a synthetic blazed grating, an Elaphe and a Xenopeltis snake shed sample patch. We compared the resulting response against the response resulting by the grating equation, which models the relationship between the grating spacing and the angles of the incident and diffracted beams of light. Figure ?? illustrates the geometrical setup for our evaluation approach: A monochromatic beam of light with wavelength λ hits a surface with periodicity d at an angle θ relative to the normal n along its incident plane. The beam emerges from the surface at the angle ϕ .

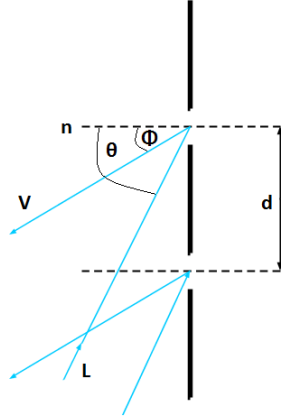


Figure 1.8: Reflecting grating: When the incident light direction is not parallel to its axis at the grating, there is another $\sin(\phi)$ involved. See also the grating equation ??.

The maximum in intensity is given by the grating equation derived from the equation ?? following figure ??:

$$\sin(\theta) = \sin(\phi) + \frac{m\lambda}{d} \quad (1.2)$$

In our evaluation we are interested in the first order diffraction, i.e. m equals one which. We further assume that the incident light direction ω_i is given. In contrast the direction of the reflected wave ω_r is not given. In Mathematics, a three dimensional direction vector is fully defined by two angles, i.e. it can be represented by spherical coordinates with radius $r = 1$. By convention, we denote those two vectors by θ and ϕ like in figure ?? . Hence, θ_i , ϕ_i and ϕ_r are given constants whereas θ_r is a free parameter for our evaluation simulation. Therefore, we are going to compare the maxima for peak viewing angles corresponding to each wavelength using data produced by our method against the maxima resulting by the grating equation ??.

1.3.1 Precomputation

For evaluation purposes we have implemented our BRDF models in java. We once again use our geometrical setup as illustrated in figure ?? where θ_i , ϕ_i and ϕ_r are provided as input values and θ_r is a free parameter. Within our evaluation we have set them to $\theta_i = 75$ $\phi_i = 0$ $\phi_r = 180$ degrees. The wavelength space Λ and the range Θ of our free parameter θ_r are discretized in equidistant steps whereas their step sizes are given as input arguments for our Java program:

$$\Lambda = \{\lambda | \lambda = \lambda_{min} + k \cdot \lambda_{step}, \quad k \in \{0, \dots, C - 1\}\} \quad (1.3)$$

where $\lambda_{step} = \frac{\lambda_{max} - \lambda_{min}}{C - 1}$ and C is the discretisation level of the lambda space. We similarly discretise the angle space by predefining an minimal and maximal angle boundary and $ceil(angMax - angMin) / angInc$ is the number of angles. Our Java BRDF model implementations are applied on the grid $[\Lambda, \Theta]$ and will store their spectral response in a matrix

$$R = \{response(\lambda_i, \theta_j) | i \in Index(\Lambda), \quad j \in Index(\Theta)\} \quad (1.4)$$

We will plot this matrix and compare its graph against the grating equation for similar condition like in stated in algorithm ??.

Algorithm 1 Vertex diffraction shader

load matrix R ??

$\lambda_{count} = |\Lambda|$

$\lambda_{inc} = \frac{\lambda_{max} - \lambda_{min}}{\lambda_{count}}$

$\lambda = \lambda_{min} + \lambda_{inc} \cdot (-1 + [1 : \lambda_{count}])$

$[maxCmaxI] = max(R)$

$viewAngForMax = angMin + angInc \cdot (maxI - 1)$

$thetaV = asin\left(\frac{\lambda}{d} - \sin\left(\frac{\theta_i \pi}{180}\right)\right) \cdot \frac{180}{\pi}$

$plot(\lambda, viewAngForMax)$

$plot(\lambda, thetaV)$

▷ graph resulting by our brdf model

▷ graph resulting by grating equation

1.3.2 Evaluation graphs

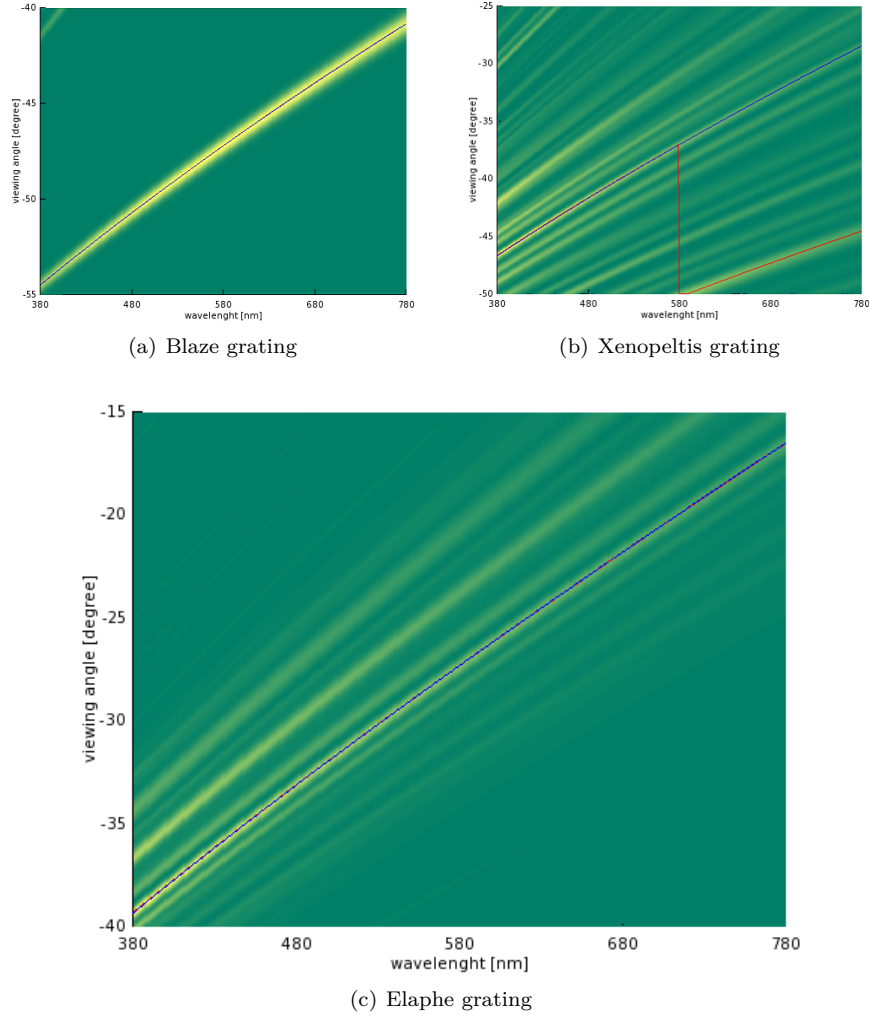


Figure 1.9: Reflectance obtained by using the shading approach described in algorithm 3 simulating a BRDF which models the effect of diffraction at different viewing angles over the spectrum of visible light.

In this section we discuss the quality of our BRDF models applied to different surface structures. For that purpose we compare the resulting relative reflectance computed as described in section ?? for each of our BRDF models to the idealized grating equation ??.

Patch	Mean[mm]	Variance[mm]
Blazed grating 2.2(a)	2500.34	0.16
Elaphe grating 2.2(b)	1144.28	0.15
Xenopeltis grating 2.2(c)	1552.27	0.45

Table 1.1: Statistics of periodicity d of our used gratings 2.2 estimated by using the grating equation ???. This table was provided by Mr. D.Singh.

Figure ?? shows the reflectance graphs resulting by the shading approach of sampling the whole lambda space described in algorithm 3. This evaluation has been applied to different idealized periodic structures, namely to the Blaze- ??, Elaphe- ?? and Xenopeltis grating ??, using an illumination angle $\theta_i = 75$ degrees. Note that higher response values are plotted in yellow and lower values in green. For each of the graphs we determine the viewing angles with peak reflectance for various wavelengths and then plot this peak viewing angles against their wavelength as solid red curves. The blue curve represents diffraction angles for an idealized periodic structure with a certain periodicity d according to the grating equation ??. The corresponding periodicity for every grating structure is estimated using the precomputed response data using again the grating equation and are tabulated in table ??.

The red and blue curve are closely overlapping in our figures ?? and ??. For Blaze and Elaphe there is only diffraction along only along one direction perceivable. Since the Blazed grating is synthetic we use its exact periodicity to plot the blue curve instead of estimating it. The Xenopeltis grating is evaluated just along the direction for the finger like structures. For Xenopeltis it is interesting to see that the red curve for the peak viewing angle toggles between two ridges corresponding to two different periodicities. this happens because there are multiple sub regions of the nanostructure with slightly different orientations and periodicity. Each sub region carves out a different yellowish ridge. depending on the viewing angle, reflectance due to one such subregion can be higher than from the others.

Figure ?? shows the evaluation plots for the (N_{min}, N_{max}) shading approach which integrates over a reduced wavelength spectrum applied to the Blaze- ?? and the Elaphe-grating ??. This optimization approach is mentioned within the discussion section of the implementation chapter 1.5 as a run-time complexity enhancement of the whole lambda space sampling approach ??. The response curve again closely matches the corresponding grating equation curve for both evaluation graphs and also look similar to the corresponding evaluation plots when integrating over the whole lambda space shown previously in figure . Therefore we may assume this optimization to be valid.

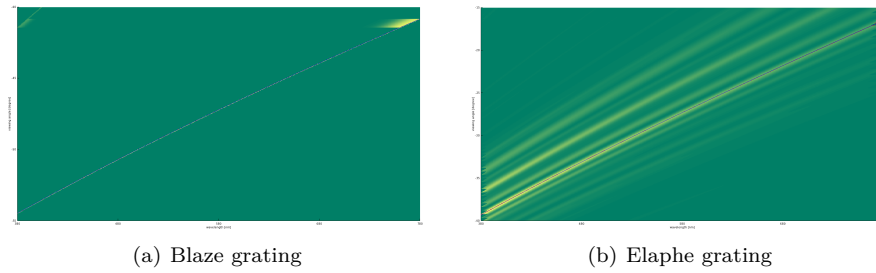


Figure 1.10: Reflectance obtained using $N_{min}N_{max}$ optimization approach

Last let us consider the evaluation graphs of the PQ approach 5 in figure ??. The PQ approach assumes the given grating being periodically distributed on a shape's surface. For this approach

we have plotted evaluation graphs of the Blaze- ?? and Elaphe grating ??. For both graphs their response curves have some similarities but also some differences compared to their corresponding grating equation curve. We could say that the response curve of the blaze grating is weakly oscillating around the grating equation curve (blue) but basically following it even there are some outliers. The response curve of the Elaphe grating is not following its corresponding first order grating equation curve rather another response curve for the PQ approach. This could be due to the assumption of the PQ approach that a given patch must be periodically distributed along the surface which is actually not that case. Nevertheless, the red curve fits one of the response curves.

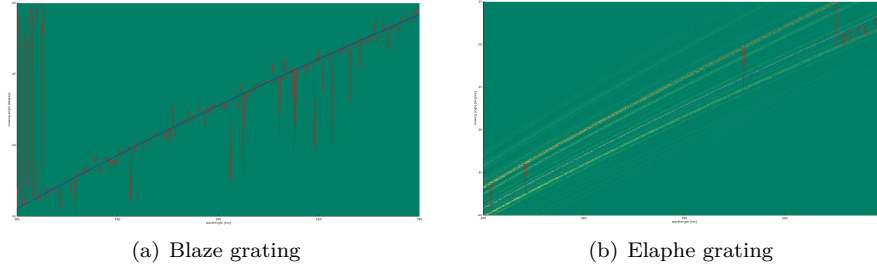


Figure 1.11: Reflectance obtained using PQ optimization approach

List of Tables

2.1	Hardware specifications of the machine which produced rendered results. Statistics are provided using the tool NVIDIA Geforce Experience.	32
-----	---	----

List of Figures

1.1	DFT Terms for a Blazed grating	5
1.2	Renderer Architecture	6
1.3	Triangular Mesh	7
1.4	Camera Coordinate System	9
1.5	Camera Matrix	9
1.6	Rays of a Directional Light	11
1.7	Triangle Rasterization	12
1.8	Lookup DFT Coefficients in Textures	16
2.1	BRDF maps for different patches: $\Theta = (\theta, \phi)$ is the direction of light propagation .	23
2.2	Cutouts of our nano-scaled surface gratings used for rendering within our shader with a scale indicator (red line) for each patch. Note that for rendering we use larger patches.	24
2.3	BRDF maps for different patches	25
2.4	BRDF maps for Blazed grating comparing our different rendering approaches . . .	25
2.5	Blazed grating at $2.5\mu m$: Different λ step sizes	26
2.6	Elaphe grating at $65\mu m$: Different λ step sizes	27
2.7	Blazed grating: PQ approach vs full lambda space sampling	27
2.8	Elaphe grating: PQ approach vs full lambda space sampling	28
2.9	Xeno grating: PQ approach vs full lambda space sampling	29
2.10	Blazed grating at $2.5\mu m$: Different σ_s sizes	30
2.11	Blazed grating at $2.5\mu m$: N Taylor Iterations	31
2.12	Elaphe grating at $65\mu m$: N Taylor Iterations	31
2.13	BRDF maps for Xeno grating: different θ_i angles	31
2.14	Diffraction of different snake skin gratings rendered on a snake geometry	33
2.15	Diffraction for Elaphe snake skin	34
2.16	Diffraction for Xeno snake skin	35
2.17	Diffraction on Elaphe snake skin grating: Different camera zoom levels	36
2.18	Diffraction on Elaphe snake skin grating: Different light directions	37
2.19	Diffraction Elaphe: experimental setup	37

List of Algorithms

1	Precomputation: Pseudo code to generate Fourier terms	4
2	Vertex diffraction shader pseudo code	10
3	Fragment diffraction shader pseudo code	14
4	Texture Blending	18
5	Sinc interpolation for PQ approach	20

Bibliography

- [Bar07] BARTSCH, Hans-Jochen: *Taschenbuch Mathematischer Formeln*. 21th edition. HASNER, 2007. – ISBN 978–3–8348–1232–2
- [CT12] CUYPERS T., et a.: Reflectance Model for Diffraction. In: *ACM Trans. Graph.* 31, 5 (2012), September
- [DSD14] D. S. DHILLON, et a.: Interactive Diffraction from Biological Nanostructures. In: *EUROGRAPHICS 2014/ M. Paulin and C. Dachsbacher* (2014), January
- [For11] FORSTER, Otto: *Analysis 3*. 6th edition. VIEWEG+TEUBNER, 2011. – ISBN 978–3–8348–1232–2
- [I.N14] I.NEWTON: *Opticks, reprinted*. CreateSpace Independent Publishing Platform, 2014. – ISBN 978–1499151312
- [JG04] JUAN GUARDADO, NVIDIA: Simulating Diffraction. In: *GPU Gems* (2004). <https://developer.nvidia.com/content/gpu-gems-chapter-8-simulating-diffraction>
- [LM95] LEONARD MANDEL, Emil W.: *Optical Coherence and Quantum Optics*. Cambridge University Press, 1995. – ISBN 978–0521417112
- [MT10] MATIN T.R., et a.: Correlating Nanostructures with Function: Structural Colors on the Wings of a Malaysian Bee. (2010), August
- [PAT09] PAUL A. TIPLER, Gene M.: *Physik für Wissenschaftler und Ingenieure*. 6th edition. Spektrum Verlag, 2009. – ISBN 978–3–8274–1945–3
- [PS09] P. SHIRLEY, S. M.: *Fundamentals of Computer Graphics*. 3rd edition. A K Peters, Ltd, 2009. – ISBN 978–1–56881–469–8
- [R.H12] R.HOOKE: *Micrographia, reprinted*. CreateSpace Independent Publishing Platform, 2012. – ISBN 978–1470079031
- [RW11] R. WRIGHT, et a.: *OpenGL SuperBible*. 5th edition. Addison-Wesley, 2011. – ISBN 978–0–32–171261–5
- [Sta99] STAM, J.: Diffraction Shaders. In: *SIGGRAPH 99 Conference Proceedings* (1999), August
- [T.Y07] T.YOUNG: *A course of lectures on natural philosophy and the mechanical arts Volume 1 and 2*. Johnson, 1807, 1807

Erklärung

gemäss Art. 28 Abs. 2 RSL 05

Name/Vorname:

Matrikelnummer:

Studiengang:

Bachelor ☐ Master ☐ Dissertation ☐

Titel der Arbeit:

.....

.....

LeiterIn der Arbeit:

.....

Ich erkläre hiermit, dass ich diese Arbeit selbständig verfasst und keine anderen als die angegebenen Quellen benutzt habe. Alle Stellen, die wörtlich oder sinngemäss aus Quellen entnommen wurden, habe ich als solche gekennzeichnet. Mir ist bekannt, dass andernfalls der Senat gemäss Artikel 36 Absatz 1 Buchstabe o des Gesetzes vom 5. September 1996 über die Universität zum Entzug des auf Grund dieser Arbeit verliehenen Titels berechtigt ist.

.....

Ort/Datum

.....

Unterschrift